






Article

RFP-MSR Hybrid Reactor Model for Tritium Breeding and Actinides Transmutation [†]

Stefano Murgo ^{1,2,*}, Chiara Bustreo ³, Marco Ciotti ⁴, Guglielmo Lomonaco ^{2,5,*}, Francesco Paolo Orsitto ⁴, Roberto Piovan ^{3,6}, Nicola Pompeo ¹, Giovanni Ricco ^{2,‡}, Marco Ripani ² and Fabio Panza ^{2,4,*}

¹ Department of Industrial, Electronic and Mechanical Engineering, Università degli studi Roma Tre, 00146 Roma, Italy; nicola.pompeo@uniroma3.it

² INFN, Sezione di Genova, 16146 Genova, Italy; marco.ripiani@ge.infn.it (M.R.)

³ Consorzio RFX, 35127 Padova, Italy; chiara.bustreo@igi.cnr.it (C.B.); roberto.piovan@igi.cnr.it (R.P.)

⁴ ENEA-Dipartimento FSN, 00044 Frascati, Italy; marco.ciotti@enea.it (M.C.); fporsitto@gmail.com (F.P.O.)

⁵ GeNERG, DIME, Università di Genova, 16145 Genova, Italy

⁶ CNR-ISTP, 20125 Padova, Italy

* Correspondence: stefano.murgo@uniroma3.it (S.M.); guglielmo.lomonaco@unige.it (G.L.);

fabio.panza@enea.it (F.P.)

[†] This paper is an extended version of our work presented at IAEA Fusion Energy Conference 2023 (FEC2023, London, UK, 16–21 October 2023) “RFP-SSR Hybrid reactor model for actinides transmutation and tritium breeding studies”.

[‡] Deceased.

Abstract: The studies on the development of fusion–fission hybrid reactors (FFHR) have gained consensus in recent years as an intermediate step before fusion energy. This work proposes a possible approach to FFHRs based on the coupling of a Reversed Field Pinch fusion machine and a Molten Salt Subcritical fission test bed. The proposed test bed is characterized by the coexistence of a fast-neutron fission core and a dedicated thermal-neutron zone, allowing the performing of tritium breeding and actinides transmutation studies. The neutronic design solutions and the results obtained by the irradiation of FLiBe salt (inside the thermal-neutron zone) and of an actinide target (inside the core) are shown. The outcomes of the analysis reveal the potential of FFHR systems as breeding/burner systems. In particular, the results regarding tritium breeding are very encouraging as the system is demonstrated to be able to reach a very high Tritium Breeding Ratio.

Keywords: fusion–fission hybrid reactors; tritium breeding; nuclear waste conversion



Citation: Murgo, S.; Bustreo, C.; Ciotti, M.; Lomonaco, G.; Orsitto, F.P.; Piovan, R.; Pompeo, N.; Ricco, G.; Ripani, M.; Panza, F. RFP-MSR Hybrid Reactor Model for Tritium Breeding and Actinides Transmutation. *Energies* **2024**, *17*, 2934. <https://doi.org/10.3390/en17122934>

Academic Editors: Sung Joong Kim and Jingen Chen

Received: 29 April 2024

Revised: 30 May 2024

Accepted: 11 June 2024

Published: 14 June 2024



Copyright: © 2024 by the authors. Licensee MDPI, Basel, Switzerland. This article is an open access article distributed under the terms and conditions of the Creative Commons Attribution (CC BY) license (<https://creativecommons.org/licenses/by/4.0/>).

1. Introduction

The development of fusion–fission hybrid reactors (FFHR) [1], an old idea proposed together with pure fusion, has seen an increasing consensus in recent years [2]. It can be considered an intermediate step before fusion energy since it requires a reduced power (about some tens of MW) D-T reactor to produce high energy (14.1 MeV) neutrons to irradiate fissile fuel [3]. Through this process, the applications are multiple: nuclear waste burn-up, fertilization of thorium or uranium for nuclear fuel production, energy generation, tritium breeding for future fusion reactors, and radioisotope production for medical applications [4–7]. The less stringent parameters of the low-power fusion reactors in hybrid systems with respect to pure fusion ones and the availability of a controlled source of high-energy neutrons to irradiate the high Z nuclear materials make this solution very attractive.

Fusion systems are generally designed for stand-alone energy generation applications, while, in the case of an FFHR, the fusion machine works as a neutron generator. Consequently, FFHRs could also represent a possible application for fusion models which are not considered to be the energy generator of the future.

In our previous studies [8], the possibility of using such systems as nuclear waste burners or converters was investigated. The proposed FFHR was composed of a coupling of a Reversed Field Pinch (RFP) [9] fusion reactor and a Stable Salt fission Test Bed (SSTB), inspired by Moltex Energy Stable Salt Reactor [10], which is an unconventional Molten Salt Reactor (MSR). Both RFP and SSTB show interesting characteristics as hybrid reactor components:

- RFP: relative design simplicity (no additional heating systems, toroidal winding at low magnetic field/room temperature), not prone to plasma disruption, and low recovery time;
- SSTB: simple design and atmospheric pressure operation;

RFP-driven FFHR is an innovative idea which could also represent a possible application of RFP systems in addition to stand-alone energy generation. A recent work about RFP neutron source application is described in [11].

The high safety margins guaranteed by an FFHR enable us to consider more complex configurations. In this work, a possible evolution of the FFHR design described in [8] is presented. The main difference is the addition of a thermal neutron spectrum zone, which led to some design choices that will be described in the following sections for different applications, including efficient tritium breeding.

Nuclear waste storage and tritium supply are two of the most relevant issues regarding fission and fusion energy, respectively. The long-term solution designed for HLW is their storage in permanent disposals, but only a few countries have already built such infrastructures [12]. On the other hand, tritium is currently generated in CANDU reactors, but its future supply is subjected to many uncertainties [13]. So, some alternative or support solutions to the current ones could have an important role in future nuclear system development.

This work provides a proposal for a conceptual design of an innovative RFP-driven FFHR and an approach to the analysis of tritium breeding via lithium conversion and actinides transmutation potential. Design choices and conversion analysis results will be shown in the following section.

2. RFP-Driven Hybrid

The main research lines for the development of the FFHR considered up to now are referred to as Tokamaks or Gas Dynamic Trap (GDT), a version of magnetic mirrors [14,15]. The recent improvements in the experimental machines and the deeper understanding of the RFP physics like the dynamics of the MHD modes, transport, and plasma wall interaction, make the RFP configuration very attractive as high-energy neutron source [16].

The main advantages of this fusion core with respect to the currently prevailing ones are as follows:

- The internal toroidal field is self-generated by the current flowing in the plasma, allowing the use of “light” room temperature toroidal field coils rated for hundreds of mT;
- No intrinsic current limit exists, so by increasing the plasma current, the ignition could be achievable through ohmic heating only, avoiding the use of additional heating systems;
- The configuration is not prone to plasma disruption.

In principle, the need for a divertor could be avoided, further simplifying the machine design. However, until now, a price has to be paid in terms of a partly chaotic character of the magnetic field leading to poorer plasma confinement with respect to Tokamaks, so the path towards realizing a power fusion reactor is more difficult; however, the confinement properties are within reasonable values for an RFP fusion core of a hybrid reactor.

In order to cover the gap between the present status of the RFP as a fusion core and the knowledge necessary in designing a full-power FFHR, a pilot FFHR based on an RFP

operating with an energy gain Q close to one has been conceived and the feasibility studies are underway [8]. The conceptual design is shown in Figure 1.

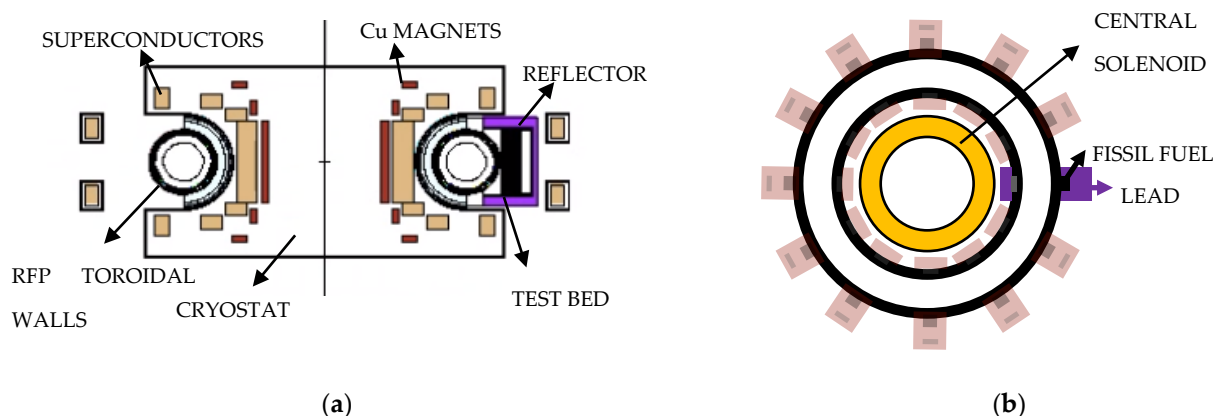


Figure 1. (a) Side view of the FFHR; (b) top view of the FFHR (RFP and test beds).

Based on the available scaling laws derived from the experimental results of the RFX-mod machine and considering the expected performance improvements in the underway machine upgrade, the main dimensions and expected performances of the fusion core are summarized in Table 1.

Table 1. Main data of the pilot RFP FFHR.

Major plasma radius [m]	4
Minor plasma radius [m]	0.8
Max plasma current [MA]	12
Electron/ion temperature [keV]	9.4
Input ohmic power [MW]	60
Fusion power [MW] ($n/n_G = 0.3$)	55
Neutron emission [10^{19} s^{-1}]	1.89
Continuous duty cycle [s]	11 ON/19 OFF

3. Neutronic Setup and Codes Coupling

The MCNP 6.1 [17] software was used to perform neutronic computations. An SDEF card was used to define the neutron source as uniformly distributed inside the plasma chamber of the RFP reactor. The neutron source is set to 1.89×10^{19} n/s. The library cross-section used for MCNP computation was the ENDF/BVII.0. MCNP computes various features such as the neutron flux in different points of the system, the energy generation, the radiation energy deposition, and so on. The results were used as inputs for FISPACT-II [18] computations.

FISPACT-II was used for inventory computations. It needs the neutron flux and spectrum at the conversion zone and the target isotopic composition as inputs. The first two are provided by MCNP computation (mean neutron flux in volume cell). As an approximation, neutron flux and spectrum were considered constant in time. These approximations are reasonable since isotope transmutation has been studied in zones where the neutron flux is imposed (i.e., can be considered constant after appropriate refueling). FISPACT has various outputs such as target isotope composition evolution, ingestion and inhalation dose computations, and decay energy. The relevant results are shown in the following section.

The computing resources and the related technical support used for this work have been provided by CRESCO/ENEAGRID High-Performance Computing infrastructure and its staff [19]. CRESCO/ENEAGRID High-Performance Computing infrastructure is funded by ENEA, the Italian National Agency for New Technologies, Energy and Sustainable Economic Development, and by Italian and European research programs (see <http://www.cresco.enea.it/english>, accessed on 1 June 2024 for further information).

4. Test Bed Design

The first version of the FFHR machine described in this work was presented at the Technical Meeting on Synergies between Nuclear Fusion Technology Developments and Advanced Nuclear Fission Technologies (Vienna, Austria 6–10 June 2022) [8]. The FFHR had a fast neutron spectrum test bed inspired by Moltex Energy Stable Salt Reactor design, a pool-type reactor with conventional-like fuel rods filled with molten salt and surrounded by molten salt coolant. The main goal of the test bed design was to evaluate the potential of the system as an actinides “burner”. The Moltex Energy SSR is an unconventional MSR since the nuclear fuel is stable (i.e., not circulating), unlike usual MSR designs. Application of such type of reactors in FFHR is interesting due to their demonstrated capability to allow high power density, reducing the space requirements.

The goal of the present work is to introduce an FFHR conceptual design feasible for high tritium breeding performances, hence some changes have been made considering the limited dimensions in which the test bed fission core will be inserted. The advantage of using an FFHR with respect to a pure fusion reactor for tritium breeding lies in the neutron multiplication occurring in the subcritical test bed. For example, if $k = 0.97$, the subcritical multiplication of the neutron flux amplitude is $M = 1/(1 - k) = 33.3$. This is a fundamental aspect because FFHR represents a strong multiplying system generating neutrons with an average energy of about 2 MeV (easier to slow down in the tritium production blanket).

Introducing the physics behind lithium and transmutation, it is possible to point out that the following:

- Tritium breeding is favored by thermal neutron irradiation because the $\text{Li}^6(n,T)\alpha$ reaction cross-section increases as the neutron energy decreases;
- Actinide burning is favored by fast neutron irradiation as the ratio between fission and capture cross-sections tends to increase proportionally to neutron energy.

Figure 2 shows the relevant cross-sections for the two cases. Am-241 behavior (Figure 2a) is representative of all HLW isotopes. Figure 2b shows the cross sections for the tritium breeding reactions from Lithium $\text{Li}^6(n,T)\alpha$ and $\text{Li}^7(n,n+T)\alpha$. As it can be seen, the $\text{Li}^6(n,T)\alpha$ reaches very high values for thermal incident neutrons: $\sigma(1 \text{ eV}) \approx 1000$ barn, while $\sigma(1 \text{ MeV}) \approx 1$ barn so that there is a factor ≈ 1000 between fast reaction and thermal reaction rate; this represents a great advantage despite of the Li^6 isotopic abundance. As an example, even considering a loss of two orders of magnitude of neutron flux amplitude during the moderation process, the worth of introducing thermalization is about 10. Multiplying and slowing down neutrons seem to be a promising technique to increase tritium breeding.

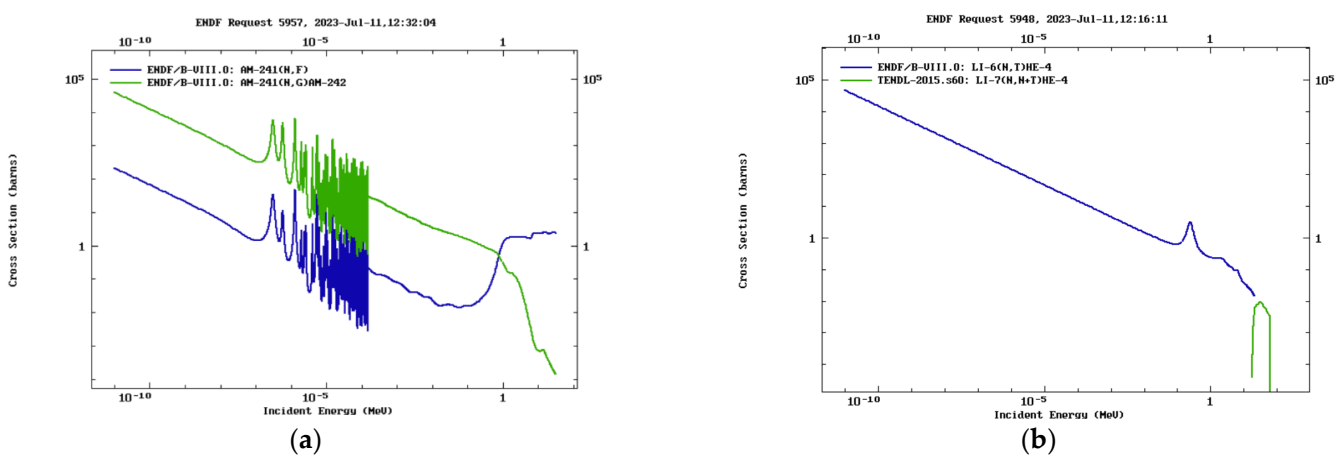


Figure 2. (a) Fission (blue) and capture (green) cross-section of Am-241; (b) tritium breeding cross-sections for Li-6 (blue) and Li-7 (green).

The FFHR test bed proposed in this study is characterized by the presence of two different zones: a subcritical fast-neutron spectrum fissile core; a thermal-neutron spectrum zone for tritium breeding analysis. The fact that the fission core is characterized by a fast neutron spectrum brings some advantages. Less nuclear waste is produced, and the core could work, in principle, as a waste burner. Figure 3 and Table 2 show the main data and the conceptual design of the fission test bed.

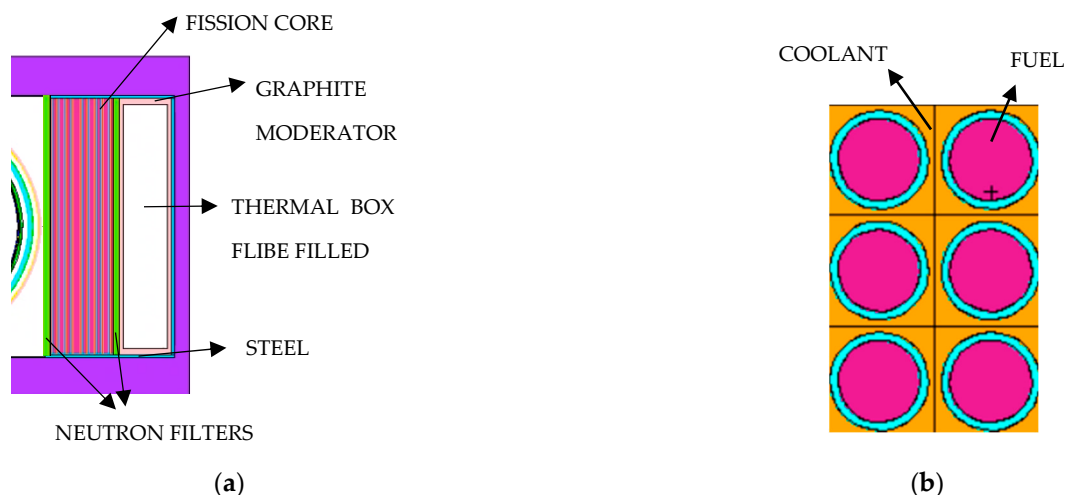


Figure 3. (a) Side view of the test bed; (b) fission core detail.

Table 2. Main data of fission test bed.

Thermal PowerPick [MWth]	≈30
Core Dimensions [cm × cm] (radial × toroidal)	50 × 110
Active Height [cm]	197
Fuel Rod Radius [cm]	0.6
Cladding Thickness [cm]	0.1
k	≈0.97
Rods pitch [cm]	1.62
Fuel	22% PuO ₂ (56% Pu ²³⁹)–77% UO ₂
Coolant	MgCl ₂ -NaCl
Reflector	Lead
Reflector Thickness [cm]	30 (lateral sides), 10 (box side)
Thermal Box Moderator	Graphite
Moderator Thickness [cm]	3
Material inside the thermal box	FLiBe (40% Li ⁶ enriched)
Thermal box width [cm]	30
Neutron Filter	Tungsten
Neutron Filters Thicknesses [cm]	0.5 (RFP side), 2 (box side)

The subcritical core has a pool-type design with salt coolant, inspired by the SSR concept proposed by Moltex Energy [3], but the limited space availability (due to the presence of the thermal zone) allows us to consider a denser ceramic fuel (MOX) instead of the molten salt fuel designed for SSRs. The fuel is inserted in conventional fuel rods as in PWRs. The power output for the test bed core turned out to be ≈ 30 MW_{th}. The test bed is, therefore, an MSR-cooled system.

A fraction (as high as possible) of the neutrons produced by the core enters a moderating zone (thermal neutron zone) for tritium breeding. The thermal-neutron zone consists of a graphite-covered box filled with FLiBe salt. The graphite operates as a neutron moderator, slowing down the neutrons coming from the core, to maximize the tritium production. The scattering cross-section of graphite increases as the neutrons' energy decreases.

The main issue regarding a thermal-neutron zone is the power excursion among the outer rods of the core, placed in front of the moderator. In fact, the reflection generates a

thermal tail in the neutron flux spectrum, increasing the fission rate. Therefore, a thermal neutron absorber is needed to avoid this undesired effect (see Figure 4a). This layer must work as a membrane substantially transparent to fast neutrons and absorbing thermal ones, similar to a high-pass filter (the analogy is very consistent since neutrons can be interpreted as waves and their energy as frequency). A similar issue, solved in the same way, appeared to exist for the fuel rods close to the RFP device because of the energy degradation of the source neutrons occurring during the transfer through the various layers of the machine. The chosen material for the filtering layers is tungsten as its absorbing cross-section matches the desired parameters.

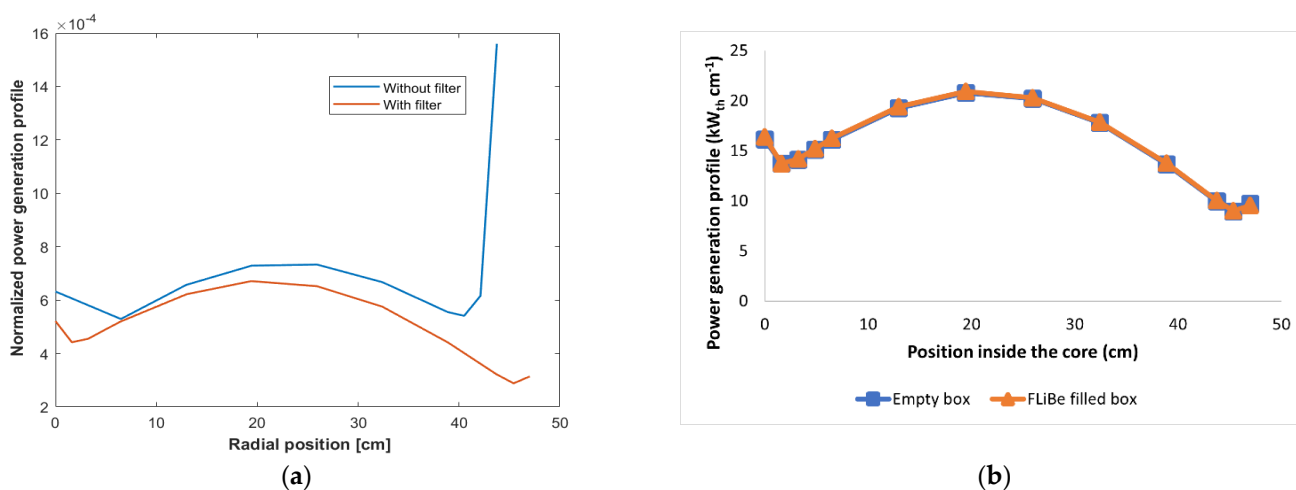


Figure 4. (a) Normalized power generation profile with and without filters; (b) power generation profile with FLiBe filled and empty box.

One of the most interesting results obtained is that the core and the graphite box are isolated from the neutronic point of view as neutrons hardly escape from the thermal zone. This feature is due to two factors:

- The presence of the tungsten neutron filter which absorbs backscattered neutrons;
- Neutrons entering the thermal zone are fast and the scattering cross-section leads to a relatively high mean free path that allows the path through the graphite. Once inside, neutrons are thermalized, their scattering cross-section increases, and the mean free path decreases so that they are somewhat trapped inside the box

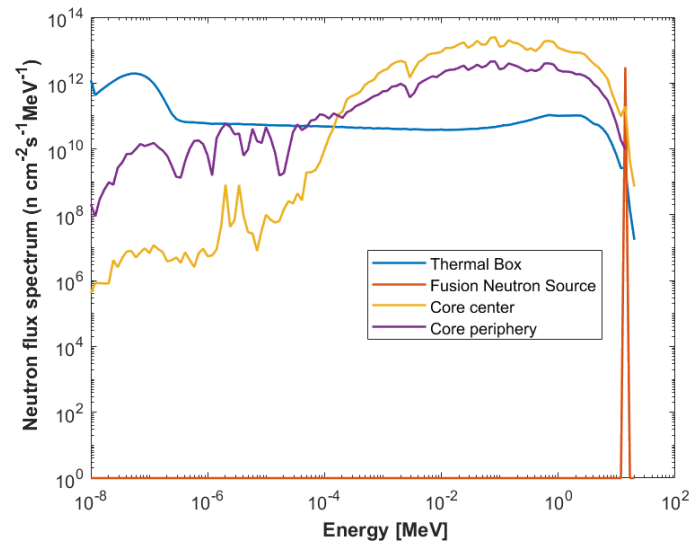
The consequence is that the presence (or absence) of the FLiBe salt inside the box does not affect the power generation profile of the core (see Figure 4b). In fact, since neutrons can hardly reenter inside the core once in the thermal zone, they must be considered lost in any case for the reactivity computations. This represents an interesting safety feature of the system.

Table 3 shows the neutron balance analysis for each zone which could give an overall picture of the neutron economy performance. The symbol “< >” indicates the cross-section values to be weighted through the neutron flux spectrum.

A comparison of the neutron flux spectra at the previously mentioned zones of the reactor is shown in Figure 5. It is possible to recognize the 14.1 MeV component given directly by the neutron source ($1.26 \times 10^{13} \text{ cm}^{-2} \text{ s}^{-1}$) and how the spectrum acquires a predominant fission distribution inside the core ($1.73 \times 10^{14} \text{ cm}^{-2} \text{ s}^{-1}$). The multiplication factor of the source given by the fission core (about 30) enables a high thermalization of the neutrons with an increase in the intensity of the flux (from 1.26×10^{13} to $2.61 \times 10^{13} \text{ n cm}^{-2} \text{ s}^{-1}$) despite the reduction due to the slowing down process. Without the fission multiplication gain, at least an order of magnitude would be lost during the moderation process. Neutron balance and cross-sections can give a clear idea about how the high TBR value (about 5) has been evaluated.

Table 3. Neutron balance of the FFHR test bed.

Zone		
SOURCE	Neutron source [10^{19} n s^{-1}]	1.89
	Neutron flux at the first wall [$10^{13} \text{ cm}^{-2} \text{ s}^{-1}$]	1.26
CORE	Mean neutron flux inside the fast core [$10^{13} \text{ cm}^{-2} \text{ s}^{-1}$]	13.01
	Neutron flux at the core center [$10^{13} \text{ cm}^{-2} \text{ s}^{-1}$]	35.35
	Maximum neutron flux at the core periphery [$10^{13} \text{ cm}^{-2} \text{ s}^{-1}$]	17.30
	$\frac{\langle \sigma_{\text{fiss}}^{\text{Pu}239} \rangle (E > 1\text{keV})}{\langle \sigma_{\text{fiss}}^{\text{Pu}239} \rangle (E < 1\text{keV})}$ at the core center	11.24
	$\frac{\langle \sigma_{\text{fiss}}^{\text{Pu}239} \rangle (E > 1\text{keV})}{\langle \sigma_{\text{fiss}}^{\text{Pu}239} \rangle (E < 1\text{keV})}$ at the core periphery	1.12
	$\frac{\langle \Sigma_{\text{fiss}} \rangle}{\langle \Sigma_{\text{cap}} \rangle}$ at the core center	0.55
	$\frac{\langle \Sigma_{\text{fiss}} \rangle}{\langle \Sigma_{\text{cap}} \rangle}$ at the core periphery	0.38
THERMAL BOX	Mean neutron flux inside the thermal box [$10^{13} \text{ cm}^{-2} \text{ s}^{-1}$]	2.61
	$\langle \sigma_{\text{n} \rightarrow \text{T}}^{\text{Li}6} \rangle [\text{cm}^{-2}]$	590
	Initial tritium breeding [$10^{19} \text{ nuclei s}^{-1}$]	≈ 9.65

**Figure 5.** Neutron spectrum for the considered test bed regions: fusion core (blue), fission core center (orange), fission core periphery (grey), and thermal box for tritium breeding (yellow).

Initial thermal-hydraulics evaluations were performed to verify whether the distance between the rods (pitch) allows a coolant flow sufficient for thermal power removal. Some other thermal-hydraulics evaluations are ongoing to carry out the following:

- Add heat exchangers for the core and graphite box to the design;
- Add an air gap between the pool and the reflector to guarantee an acceptable temperature (i.e., sufficiently lower than the melting point) for the lead reflector.

5. Tritium Breeding Results

Tritium is a synthetic isotope of hydrogen, and its supply is one of the main issues regarding future fusion reactor operations. It can be produced from lithium through the following reactions (see Figure 2b):

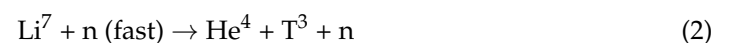
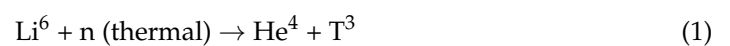


Figure 6a,b show the results obtained by MCNP (Figure 6a and FISPACT-II Figure 6b) for the graphite box. As can be seen in Figure 6a, the graphite box has a huge moderation effect on the neutron flux. The insertion of a FLiBe salt enriched at a level of 40% in Li^6 considerably reduces the thermal tail of the neutron flux spectrum, making the Li^6 reaction (Equation (1)) extremely efficient for thermal neutrons. FLiBe was chosen following the idea to use salts and because some FLiBe-based tritium blankets are cited in the literature [20,21].

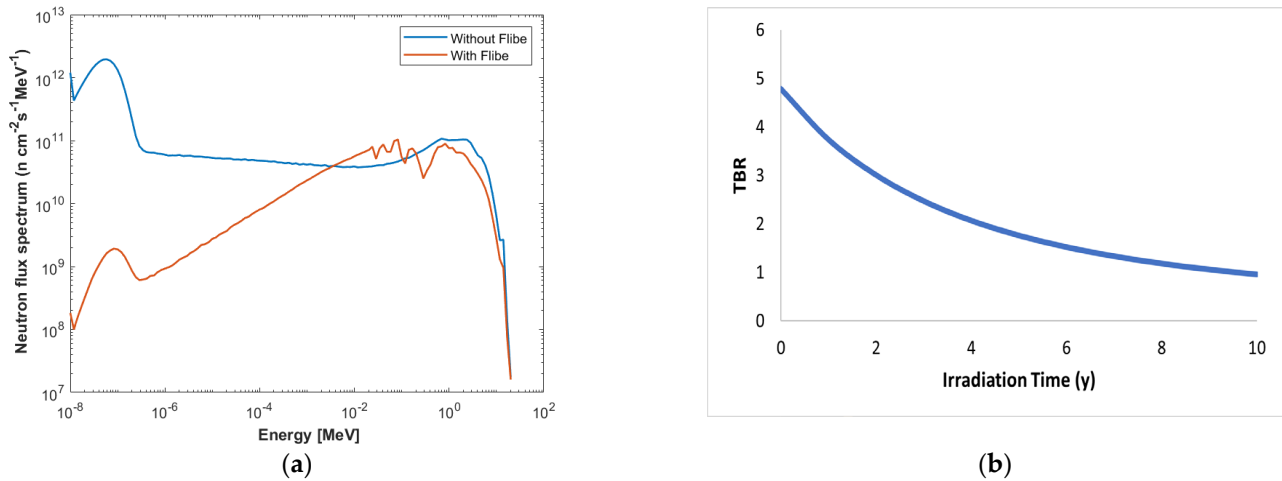


Figure 6. (a) Spectrum of the neutron flux inside the graphite filled with FLiBe and empty; (b) TBR evolution after irradiation.

Figure 6b shows the evolution of the Tritium Breeding Ratio (TBR) of the graphite box after irradiation. The TBR is defined as the ratio between the tritium mass generated by the breeding system and the tritium mass consumed by the whole fusion machine through D-T reactions:

$$\text{TBR} = \frac{\sum_i \int \Phi_{\text{Box}} \sigma_{\text{TB}}^i N_{\text{Li}}^i dV_{\text{box}}}{\frac{1}{4} n^2 \langle \sigma_f v \rangle V_{\text{pl}}} \quad (3)$$

where Φ_{Box} is the mean flux inside the thermal box, σ_{TB} is the sum of the tritium breeding cross sections, N_{Li}^i is the lithium isotope nuclear density, V_{box} is the volume of the graphite box, the index i indicates the lithium isotope, n is the plasma density, $\langle \sigma_f v \rangle$ is the average fusion cross section over the Maxwellian velocity distribution, and V_{pl} is the plasma volume. The denominator is the fusion rate and its value is set to 1.8×10^{19} reactions/s. The numerator is the tritium breeding rate, computed by FISPACT-II.

The neutron flux inside the empty box is of the order of $10^{13} \text{ n cm}^{-2} \text{ s}^{-1}$ with more than 80% of the neutrons with an energy $< 1 \text{ eV}$. Due to the high cross-section of reaction $\text{Li}^6(n, \text{T})\alpha$ in the range 0.01–1 eV (100–1000 barn), the tritium breeding rate can reach excellent performances. Figure 6a shows how FLiBe salt consumes the thermal fraction of the neutron spectrum, which is reduced to up to 4 orders of magnitude.

In this case, the TBR value decreases over time due to the Li consumption. This aspect could be managed via refueling operations, which were not the main goal of this work. It is worth noting that a tiny graphite box (30 cm wide) has an initial TBR of the order of 5 (Figure 6b). In comparison, breeding blankets designed for fusion stand-alone reactors hardly reach $\text{TBR} \approx 1$.

Promising results on tritium breeding suggest that FFHR systems could play a key role in the tritium supply chain for fusion reactors.

6. Actinides Conversion Results

Since the fission core of the proposed concept is characterized by a fast neutron spectrum, the irradiation of a nuclear waste target was also tested to understand whether the reactor could operate in the same way as a tritium breeder and an actinide convertor.

Minor actinides (nuclear waste) treatment via neutron irradiation could represent an intermediate step before storage [22,23]. The goals of an irradiation treatment are the reduction in waste mass/volume and repository lifetime.

The capability of the test bed as a waste burner/convertor was tested by inserting a 1 kg waste target composed as described in Table 4 inside the fission core. The composition of the target is derived from the isotope concentration measurements on the spent fuel of Neckarwestheim Nuclear Power Station module 2 (GKN 2, Neckarwestheim, Germany) [24].

Table 4. C Target composition.

Isotope	Mass %
Np-237	39.7%
Am-241	34.3%
Am-242	0.10%
Am-243	16.2%
Cm-243	0.05%
Cm-244	8.68%
Cm-245	0.87%

Figure 7 shows the irradiation neutron flux spectrum. It can be noted that the neutron flux spectrum is dominated by fission and no relevant thermal tail is present. Figure 8a,b show the main results of a 10-year continuous irradiation. Figure 8a shows the evolution of the composition of the target, while Figure 8b reports the evolution of the Level of Mine Balancing Time (LOMBT), i.e., the repository lifetime (technically, the time when waste level radiotoxicity matches the level relative to the mined U one) [25]. Here, LOMBT represents the relative radiotoxicity (to mined U) of actinides only, excluding the produced plutonium.

The results show that the main effect of the neutron irradiation of the actinides target appears to be the conversion of a part of neptunium and americium into plutonium (mainly Pu²³⁸ and Pu²⁴⁰). The conversion level reaches 20% of the mass of the target after the equivalent of 10 years of continuous irradiation. This can be considered a good outcome as plutonium may be reused as fuel in nuclear systems (mass recycling).

On the other hand, LOMBT is only slightly affected by irradiation. A quite relatively small reduction in the repository lifetime of 20 years is estimated after 10 years of net irradiation.

Future analysis will also regard the actinide target irradiation in the thermal box. In fact, recent studies [26] showed that low-fluence thermal neutron irradiation on HLW may lead to interesting results for waste recycling in FFHR systems.

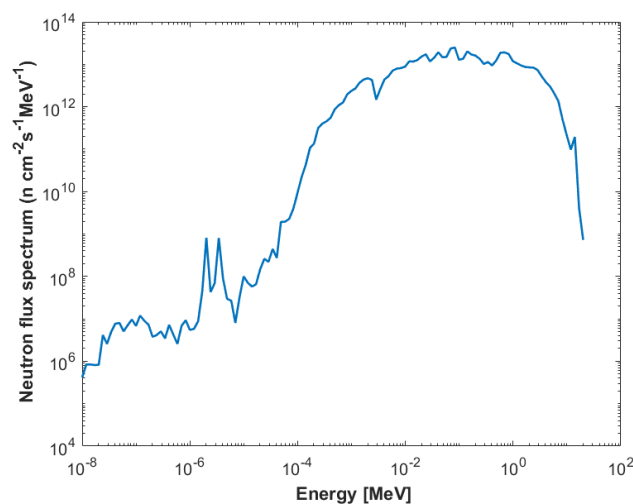


Figure 7. Actinide target irradiation neutron flux spectrum.

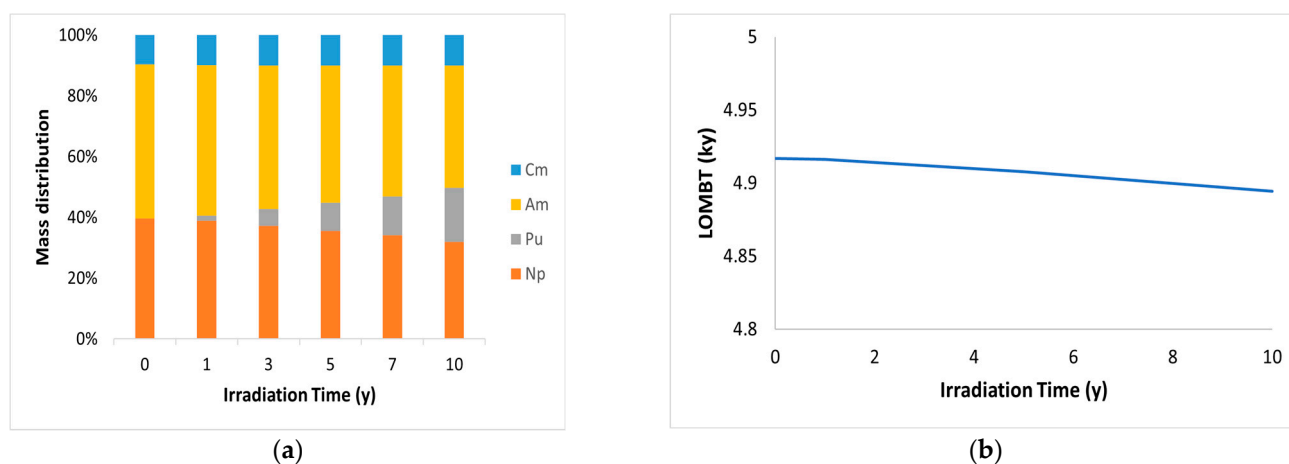


Figure 8. (a) Evolution of the mass distribution of the irradiated actinide target; (b) LOMBT evolution after target irradiation.

7. Conclusions

A two-zone FFHR test bed design has been proposed and its tritium breeding and energy generation/actinide conversion properties have been analyzed: a fast-neutron zone represents the actual subcritical fission core ($k \approx 0.97$). A nuclear waste target was inserted inside this zone to test the potential of the machine as an actinide converter; a thermal-neutron zone was designed to test the potential of the system as a tritium breeder. It has a strong thermalization power and most of the neutrons reach energies below 1 eV.

The introduction of a tungsten layer (“neutron filter”) was needed to prevent high power excursion at the interface core/thermal box (see Section 4).

FLiBe salt (40% Li^6 enriched on the total lithium mass) irradiation inside the thermal-neutron zone exhibited very encouraging results as the TBR of a single module reached a maximum value of 5. It is important to underline that, in this preliminary study, a single compact module has been used while the available RFP space can be fully covered with other test beds. The TBR value has been calculated only considering the net T production: extraction efficiency and other leaking effects have not yet been evaluated.

The results show that the transmutation of the waste target led to an actinide mass conversion of up to 20%, considering a net irradiation time of 10 years. The main effect of neutron irradiation is the conversion of americium and neptunium isotopes to plutonium ones. This can be considered a good outcome since plutonium can be reused as fuel in nuclear systems. A slight reduction in the repository lifetime was also estimated.

Future developments will regard the simulation of HLW irradiation inside the design thermal box and thermal–hydraulic evaluation for heat exchangers, component design, and space optimization. Also, chemical and mechanical stress analysis was not the object of this work but will be needed in future developments.

Author Contributions: Conceptualization, S.M., G.L., and F.P.O.; methodology, S.M. and F.P.O.; software (MCNP 6.1 and FISPACT-II 5.0), S.M. and F.P.O.; validation, S.M. and F.P.O.; formal analysis, S.M. and F.P.O.; data curation, S.M., F.P.O., R.P., and C.B.; writing—original draft preparation, S.M.; writing—review and editing, all authors; visualization, S.M., F.P.O., R.P., and C.B.; supervision, F.P.O. and N.P.; project administration, S.M., G.L., and F.P. All authors have read and agreed to the published version of the manuscript.

Funding: This research has been partially funded by the PRIN (Progetti di Ricerca di rilevante Interesse Nazionale) grant n. 2022BKEH9Y (“Fusion-fission hybrid pilot reactor for sustainable energy transition”) provided by the Italian Ministry of University and Research (MUR). The research activity of Stefano Murgo has been supported by PhD PON (Programma Operativo Nazionale) grant (“Study of Fusion Fission Hybrid System potentiality for nuclear waste transmutation and energy

sustainability”) provided by the Italian Ministry of University and Research (MUR); the PhD course is held at Roma Tre University (XXXVII cycle).

Data Availability Statement: MCNP 6.1 and FISPACT-II outputs and corresponding elaborated data can be available upon request due to legal reasons.

Conflicts of Interest: The authors declare no conflicts of interest.

References

1. Bethe, H. The fusion hybrid. *Phys. Today* **1979**, *32*, 44. [[CrossRef](#)]
2. Kuteev, B.V.; Goncharov, P.R. Fusion–Fission Hybrid Systems: Yesterday, Today, and Tomorrow. *Fusion Sci. Technol.* **2020**, *76*, 836–847. [[CrossRef](#)]
3. Freidberg, J.P.; Kadak, A.C. Fusion–fission hybrids revisited. *Nat. Phys.* **2009**, *5*, 370–372. [[CrossRef](#)]
4. Stacey, W.M.; Mandrekas, J.; Hoffman, E.A.; Kessler, G.P.; Kirby, C.M.; Mauer, A.N.; Noble, J.J.; Stopp, D.M.; Ulevich, D.S. A fusion transmutation of waste reactor. *Fusion Eng. Des.* **2002**, *63–64*, 81–86. [[CrossRef](#)]
5. Ridikas, D.; Plukiene, R.; Plukis, A.; Cheng, E.T. Fusion-fission hybrid system for nuclear waste transmutation (I): Characterization of the system and burn-up calculations. *Prog. Nucl. Energy* **2006**, *48*, 235–246. [[CrossRef](#)]
6. Khripunov, V.I.; Kuteev, B.V.; Zhirkin, A.V. Enhanced tritium production in fusion-fission hybrids for the external consumption. *Fusion Eng. Des.* **2019**, *146*, 1569–1573, ISSN 0920-3796. [[CrossRef](#)]
7. Ciotti, M.; Panza, F.; Cardinali, A.; Gatto, R.; Ramogida, G.; Lomonaco, G.; Ricco, G.; Ripani, M.; Osipenko, M. Novel hybrid pilot experiment proposal for a Fusion-fission subcritical coupled system. In *Voprosy Atomnoj Nauki I Tehniki. Seriya, Termodernyj Sintez; Problems of Atomic Science and Technology, Series Thermonuclear Fusion*; Kurchatov Institute: Moscow, Russia, 2021; Volume 44, pp. 57–64. [[CrossRef](#)]
8. Piovan, R.; Bustreo, C.; Cavazzana, R.; Cemmi, A.; Ciotti, M.; Cherubini, N.; Escande, D.E.; Gaio, E.; Lomonaco, G.; Lunardon, F.; et al. Pilot Hybrid Experiment with Reversed Field Pinch as neutron source and double test beds: An innovative stage approach towards a full power Fusion-Fission Hybrid Reactor. In Proceedings of the Technical Meeting on Synergies between Nuclear Fusion Technology Developments and Advanced Nuclear Fission Technologies, Vienna, Austria, 6–10 June 2022.
9. Marrelli, L.; Martin, P.; Puiatti, M.E.; Sarff, J.S.; Chapman, B.E.; Drake, J.R.; Escande, D.F.; Masamune, S. The reversed field pinch. *Nucl. Fusion* **2021**, *61*, 023001. [[CrossRef](#)]
10. Scott, I.; Abram, T.; Negri, O. Stable Salt Reactor Design Concept. In Proceedings of the International Thorium Energy Conference: Gateway to Thorium Energy, Mumbai, India, 12–15 October 2015.
11. Piovan, R.; Agostinetti, P.; Bustreo, C.; Cavazzana, R.; Escande, D.; Gaio, E.; Lunardon, F. Status and Perspectives of a Reversed Field Pinch as a Pilot Neutron Source. *IEEE Trans. Plasma Sci.* **2020**, *48*, 1708–1714. [[CrossRef](#)]
12. El-Showk, S. Final Resting Place. *Science* **2022**, *375*, 806–810. [[CrossRef](#)] [[PubMed](#)]
13. Pearson, R.J.; Antoniazzi, A.B.; Nuttall, W.J. Tritium supply and use: A key issue for the development of nuclear fusion energy. *Fusion Eng. Des.* **2018**, *136*, 1140–1148, ISSN 0920-3796. [[CrossRef](#)]
14. Stewart, C.L.; Stacey, W.M. The SABrR Concept for a Fission-Fusion Hybrid ^{238}U -to- ^{239}Pu Fissile Production Reactor. *Nucl. Technol.* **2014**, *187*, 1–14. [[CrossRef](#)]
15. Ivanov, A.A.; Prikhodko, V.V. Gas-dynamic trap: An overview of the concept and experimental results. *Plasma Phys. Control. Fusion* **2013**, *55*, 063001. [[CrossRef](#)]
16. Marrelli, L.; Cavazzana, R.; Bonfiglio, D.; Gobbin, M.; Marchiori, G.; Peruzzo, S.; Puiatti, M.E.; Spizzo, G.; Voltolina, D.; Zanca, P.; et al. Upgrade of the RFX-mod reversed field pinch and expected scenario improvements. *Nucl. Fusion* **2019**, *59*, 076027. [[CrossRef](#)]
17. Werner, C.J.; Armstrong, J.C.; Brown, F.B.; Bull, J.S.; Casswell, L.; Cox, L.J.; Dixon, D.A.; Forster, R.A., III; Goorley, J.T.; Hughes, H.G., II; et al. *MCNP User’s Manual Code Version 6.2*; Los Alamos National Laboratory Tech. Rep. LA-UR-17-29981; Los Alamos National Laboratory: Los Alamos, NM, USA, 2017.
18. Fleming, M.; Stainer, T.; Gilbert, M. (Eds.) *The FISPACT-II User Manual*; UKAEA-R(18)001; UKAEA, Culham Science Centre: Abingdon, Oxon, UK, 2018.
19. Iannone, F.; Ambrosino, F.; Bracco, G.; De Rosa, M.; Funel, A.; Guarnieri, G.; Migliori, S.; Palombi, F.; Ponti, G.; Santomauro, G.; et al. CRESCO ENEA HPC clusters: A working example of a multifabric GPFS Spectrum Scale layout. In Proceedings of the 2019 International Conference on High Performance Computing & Simulation (HPCS), Dublin, Ireland, 15–19 July 2019; pp. 1051–1052.
20. Forsberg, C.; Zheng, G.; Ballinger, R.G.; Lam, S.T. Fusion Blankets and Fluoride-Salt-Cooled High-Temperature Reactors with Flibe Salt Coolant: Common Challenges, Tritium Control, and Opportunities for Synergistic Development Strategies Between Fission, Fusion, and Solar Salt Technologies. *Nucl. Technol.* **2020**, *206*, 1778–1801. [[CrossRef](#)]
21. Boullon, R.; Jaboulay, J.-C.; Aubert, J. Molten salt breeding blanket: Investigations and proposals of pre-conceptual design options for testing in DEMO. *Fusion Eng. Des.* **2021**, *171*, 112707, ISSN 0920-3796. [[CrossRef](#)]
22. Salvatores, M.; Palmiotti, G. Radioactive waste partitioning and transmutation within advanced fuel cycles: Achievements and challenges. *Prog. Part. Nucl. Phys.* **2011**, *66*, 144. [[CrossRef](#)]
23. Salvatores, M. Nuclear fuel cycle strategies including Partitioning and Transmutation. *Nucl. Eng. Des.* **2004**, *235*, 805. [[CrossRef](#)]

24. Radulescu, G.; Gauld, I.C.; Ilas, G. *SCALE 5.1 Predictions of PWR Spent Nuclear Fuel Isotopic Compositions*; Oak Ridge National Laboratory: Oak Ridge, TN, USA, 2010.
25. Cerullo, N.; Bufalino, D.; Forasassi, G.; Lomonaco, G.; Rocchi, P.; Romanello, V. An additional performance of HTRS: The waste radiotoxicity minimization. *Radiat. Prot. Dosim.* **2005**, *115*, 122–125. [[CrossRef](#)]
26. Murgu, S.; Ciotti, M.; Lomonaco, G.; Pompeo, N.; Panza, F. Multi-group analysis of Minor Actinides transmutation in a Fusion Hybrid Reactor. *EPJ Nucl. Sci. Technol.* **2023**, *9*, 36. [[CrossRef](#)]

Disclaimer/Publisher's Note: The statements, opinions and data contained in all publications are solely those of the individual author(s) and contributor(s) and not of MDPI and/or the editor(s). MDPI and/or the editor(s) disclaim responsibility for any injury to people or property resulting from any ideas, methods, instructions or products referred to in the content.